Sustainable Chemistry and Pharmacy 13 (2019) 100166

Contents lists available at ScienceDirect

Sustainable Chemistry and Pharmacy

journal homepage: http://www.elsevier.com/locate/scp

# Collagen from Turkey (*Meleagris gallopavo*) tendon: A promising sustainable biomaterial for pharmaceutical use

Krister Gjestvang Grønlien [a,*], Mona Elisabeth Pedersen [b], Karen Wahlstrøm Sanden [b], Vibeke Høst [b], Jan Karlsen [a,1], Hanne Hjorth Tønnesen [a]

[a] Section for Pharmaceutics and Social Pharmacy, Department of Pharmacy, University of Oslo, P.O. Box 1068 Blindern, NO-0316, Oslo, Norway
[b] Nofima AS, P.O. Box 210, NO-1431, Ås, Norway

ARTICLE INFO

*Keywords:*
Collagen
Rest raw material
Characterization
Drug delivery

ABSTRACT

Collagen is the major fibrillar component and protein in both human and animal connective tissue. It is applied in medical preparations, e.g. wound dressings and tissue engineering. Meat and poultry production industries result in large amounts of organic waste, rich in collagen. Our aim was to isolate and characterize pepsin soluble collagen from turkey tendon. Structural analysis indicated the presence of α-chains from both collagen type I and III, β-dimers and γ-trimers, consistent with the estimated molecular weight of 477.3 kDa. Circular dichroism spectroscopy confirmed an intact triple helix. The collagen demonstrated excellent thermal stability, with denaturation temperatures ($T_{max}$) at 38.5 °C and 44.5 °C and partial refolding after extensive heating. Biocompatibility was confirmed through cell viability tests. The collagen was investigated for its potential drug carrier ability. Freeze dried collagen scaffolds containing prilocaine hydrochloride and riboflavin were prepared in the presence or absence of photo-crosslinking. Photochemical crosslinking was confirmed by SEM and enhanced mechanical properties were observed. Scaffolds had a significant slower *in vitro* release of the active ingredient than a reference solution. Altogether, our study suggests collagen from turkey tendon as a promising sustainable biomaterial for pharmaceutical use.

## 1. Introduction

Industrial production of meat and poultry products results in large amounts of organic waste. The waste is today often utilized as biofuel and in production of pet food, but also incinerated without energy recovery (Jayathilakan et al., 2012). However, there is a huge potential in the application of rest raw materials from food production industries for new and innovative purposes. Rest raw materials are defined as remains from the food production after the edible part is utilized. The increasing production and consumption of poultry, including turkey (*Meleagris gallopavo*), results in an increasing amount of rest raw material such as skin, tendons and bones i.e., materials that are rich in the protein collagen.

Collagen is the major fibrillar component and protein in both human and animal connective tissue, constituting about 20–30% of the total body protein weight. Collagen has a characteristic triple helix structure formed by three α-chains held together by hydrogen bonds in its native form. The α-chains consist of repeating triplets of the amino acids Glycine-X-Y, where X and Y are often proline and the imino acid hydroxyproline, respectively. Nonhelical telopeptides are attached to the ends of the collagen molecule. These telopeptides are the major source of antigenicity, but can be removed by pepsin digestion to produce atelocollagen, which is considered as biocompatible and is well tolerated by the human body. Collagen is classified into different types, and at least 28 variants of collagen have been identified. The types differ in origin, structure and their ability to form fibrils (Shoulders and Raines, 2009). Collagen has several potential applications in the food, medical, pharmaceutical and cosmetic industries.

Collagen from several different species has been evaluated for application in cosmetics and pharmaceutical preparations. Collagen isolated from avian sources has several beneficial properties compared to collagen from e.g. pigs, cattle and aquatic species. Due to the lack of diseases like bovine spongiform encephalopathy (BSE), transmissible spongiform encephalopathy (TSE) and foot-and-mouth disease (FMD),

* Corresponding author.
*E-mail address:* k.g.gronlien@farmasi.uio.no (K.G. Grønlien).
[1] Deceased 21 March 2019.

https://doi.org/10.1016/j.scp.2019.100166
Received 8 May 2019; Received in revised form 8 August 2019; Accepted 8 August 2019
Available online 12 August 2019

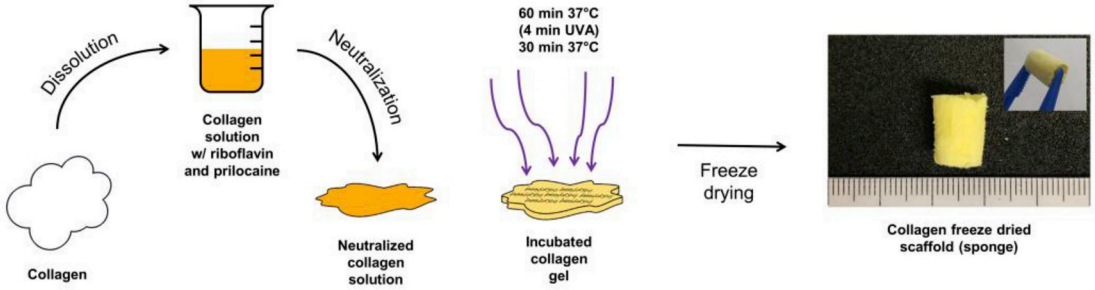


**Fig. 1.** Schematic showing the formation of the collagen freeze dried scaffolds (sponges).

avian sources can be regarded as safer than pigs and cattle although avian influenza (AI) can be a challenge (Li et al., 2004; Parenteau-Bareil et al., 2011; Pantin-Jackwood et al., 2017). Collagen is classified as "Generally Recognized as Safe" (GRAS) by the US Food and Drug Administration (FDA). There is an increasing interest for collagen from aquatic species as an alternative to collagen from mammal species, due to the various diseases and religious preferences. However, the use of aquatic collagen is limited by relatively poor thermal stability. With respect to cosmetic and medical applications, the collagen to be used should have a denaturation temperature above the human body temperature to avoid protein denaturation. Avian species are known to have a higher body temperature than mammal species, aquatic species and humans and thereby a higher denaturation temperature (Prinzinger et al., 1991; Varriale and Bernardi, 2006). Collagen from different fish species has shown a denaturation temperature $\leq$15.2 °C below mammal species (Sotelo et al., 2016). A previous study showed that pepsin soluble collagen type I isolated from quails' feet exhibited high thermal stability with a denaturation temperature of 38.3 °C, compared to calf skin (36.3 °C) and pig skin collagen (37.0 °C) (Yousefi et al., 2017). Collagen from chicken bone is reported to have a denaturation temperature at 44.0 °C, which was claimed to be the highest denaturation temperature for vertebrate collagen at the time of publication (Losso and Ogawa, 2014). The average body temperature of turkey is determined to 41.1 °C, which should indicate excellent thermal stability (Wilson and Woodard, 1955). Collagen from turkey has, however, not been thoroughly investigated for potential use in medicine or pharmacy.

Gels, sponges and shields are examples of medicinal and pharmaceutical products based on collagen. Collagen is used in tissue engineering as surgical suture, hemostatic agent, skin- and other tissue replacement (Chattopadhyay and Raines, 2014; Farndale, 2006). Collagen is known to have excellent wound healing properties because of its biocompatibility, biodegradability and chemotactic properties to cells involved in production of extracellular matrix (Chattopadhyay and Raines, 2014; Postlethwaite et al., 1978). Further, collagen can be used in the preparation of drug delivery devices. Examples are hydrogels and freeze-dried scaffolds (sponges). Hydrogels are composed of a crosslinked polymer network that contains a large amount of water. Drug molecules can be incorporated in the polymer network by covalent linkage, electrostatic interactions, hydrophobic association or by physical entrapment in the polymer network (Li and Mooney, 2016). Collagen is soluble in acids and is easily crosslinked by neutralization and self-assembly into fibrils at 37 °C. The mechanical properties and pore size of collagen hydrogels can be altered by a change in collagen concentration and further crosslinking by a chemical or photochemical process. Chemical crosslinkers like glutaraldehyde and epoxy compounds are often cytotoxic and not suitable for medicinal use. Photochemical crosslinkers are activated upon irradiation with the appropriate wavelength. Riboflavin (Vitamin $B_2$) is known to induce photochemical polymerization and interhelical crosslinking between the collagen molecules when exposed to UVA or blue light (Heo et al., 2016; Tirella et al., 2012). Riboflavin is an endogenous compound and is GRAS classified. A photochemical crosslinker can be added to the formulation at an early stage in the production. This is an advantage compared to chemical crosslinkers, which need to be added at the time of crosslinking. Collagen sponges can be formed by freeze drying of the photochemically crosslinked gels. Another approach is to stabilize and crosslink collagen with nanoparticles or make nanocomposites. This can be illustrated by the formation of novel functional biocomposites with improved surface area and porosity, like collagen sponges with iron oxide nanoparticles or iron encapsulated carbon nanoparticles for various environmental, energy and biorelated applications (Ashokkumar et al., 2016; Telay Mekonnen et al., 2019). Another example is the formation of nanocomposites with collagen and silica for wound healing (Desimone et al., 2011). Further, collagen is often used in a composite together with hydroxyapatite for bone tissue engineering (Kane et al., 2015). All of these techniques result in crosslinked materials with increased thermal properties, increased mechanical strength and improved porosity. Recently, the use of collagen alone and in polymer blends in bioinks for bioprinting and tissue engineering has gained attention. With bioprinting, the scaffold can be tailored to increase cell migration and proliferation (Rider et al., 2018).

In the present study, collagen was isolated from turkey rest raw material and characterized with respect to physicochemical properties and drug carrier ability. The biocompatibility was assessed with viability studies on human primary dermal fibroblasts treated with the isolated material. A freeze-dried scaffold (sponge) containing riboflavin as a photochemical crosslinker and prilocaine hydrochloride as a model drug was prepared (Fig. 1). The morphology was examined, and the *in vitro* release profile of the active ingredient was recorded. Our data reveal the potential for turkey tendon collagen as a promising sustainable material for drug delivery.

## 2. Materials and methods

All experiments were performed at 25 °C unless other stated.

### 2.1. Raw materials, chemicals and reagents

Rest raw material from industrially produced turkey (*Meleagris gallopavo*) was kindly provided by Norilia AS (Oslo, Norway). The raw material was stored at −20 °C until further preparation. All reagents were of analytical grade and were purchased from either Sigma-Aldrich Chemical Company (St. Louis, MO, USA) or Merck KGaA (Darmstadt, Germany). Cell medium and components were all purchased from Thermo Fischer Scientific (Waltham, MA, USA). Viability assay was purchased from Promega Corporation (Madison, WI, USA).

### 2.2. Preparation of pepsin-solubilized collagen from Turkey tendon

Frozen turkey tendons were thawed and manually cleaned with a scalpel to remove any remaining meat. The cleaned material was cut into smaller pieces and freeze dried for 48 h (Alpha 1–2 LD Plus Freeze Fryer, Martin Christ, Germany). Acetic acid solution (0.5 M) with pepsin (1:10) was added and the material was hydrolyzed enzymatically for

48 h at 4 °C with stirring. The mixture was then centrifuged at 4 °C and 20 000×*g* for 1 h (Avanti J-26 XP, Beckman Coulter, Brea, CA, USA). The supernatant was collected and transferred to new vials. NaCl (4 M) was added to the supernatant in a 1:3 ratio and kept on ice for 24 h to precipitate collagen. The solution was thereafter centrifuged at 20 000×*g* and 4 °C for 1 h and the sediment was further removed and replaced with 0.5 M acetic acid for re-solubilization. The mixture was dialyzed against distilled water for 3 days with change of medium every 24 h. The dialyzed solution was frozen to −40 °C and freeze dried for 96 h (Gamma 1–16 LSC Freeze dryer, Martin Christ, Germany).

### 2.3. Characterization of collagen

#### 2.3.1. Total collagen quantification

The concentration of collagen was measured using the Sircol™ Soluble Collagen Assay (Biocolor Ltd., Carrickfergus, UK). Colorimetric detection of collagen was performed according to the manufacturer's protocol. In brief, 1.0 ml of the dye (Sirius Red) was added to 100 µl diluted collagen solution (approximately 10 µg collagen). The solution was agitated for 30 min followed by centrifugation at 10 000×*g* for 10 min. The dye-protein complex-pellet formed was collected and washed with 750 µl of the provided Acid-Salt Wash reagent. The pellet was once again collected and dissolved in 1.0 ml of the provided alkaline solution to release the dye. The absorbance was measured at 550 nm by an UV-VIS spectrophotometer (UV–2401PC, Shimadzu, Kyoto, Japan). Reagent blank was 0.5 M acetic acid. A calibration curve was prepared using bovine collagen type I (total amount in the samples was 5–15 µg). The assay does not discriminate between the different types of collagen.

The Sircol™ dye exclusively binds to collagen and the assay was used to assess the purity of the isolated material by comparing the amount of raw material to the total collagen quantified (Fauzi et al., 2016). Collagen isolated from turkey tendon was dissolved in 20 mM acetic acid to a concentration of 1.0 mg/ml. The collagen concentration was determined by the Sircol™ Assay to assess the purity of the isolated material and the recovery of collagen after filtration (5 µm Versapor® Membrane, Pall Corporation, MI, USA).

#### 2.3.2. Collagen viscosity and molecular weight

Collagen isolated from turkey tendon was dissolved in 0.5 M acetic acid to a concentration of 0.5 mg/ml. The solution was diluted to concentrations between 0.1 and 0.5 mg/ml. Acetic acid (0.5 M) was used as negative control. The viscosity of the solutions was determined with an Anton Paar Rheometer (Anton Paar Physica MCR301 Rheometer, Germany). Samples of 10 ml were measured with a double gap concentric cylinder (DG26.7) at 25 °C with a shear rate of 10 $s^{-1}$. The intrinsic viscosity of collagen was calculated from the dynamic viscosity (Kulicke and Clasen, 2004). The average molecular weight was then estimated from the intrinsic viscosity according to the Kuhn-Mark-Houwink-Sakurada equation (Equation (1)):

$$[\eta] = KM^{\alpha} \quad (1)$$

where $\eta$ is the intrinsic viscosity, $M$ is the average molecular weight, $K$ and α are values specific for the polymer or protein ($1.86 \times 10^{-19}$ and 1.8 for collagen, respectively) (Nishihara and Doty, 1958).

#### 2.3.3. Sodium dodecyl sulphate-polyacrylamide gel electrophoresis (SDS-PAGE)

SDS-gel electrophoresis is a common method for determination of collagen polypeptide chains (Cliche et al., 2003; Rabotyagova et al., 2008). 20 µg of freeze dried collagen material was solubilized in 7 M Urea/2 M Thiourea, 2% CHAPS, 1% dithiothreitol before adding sample buffer to a final concentration of 0.05% Tris-HCl pH 6.8, 7% glycerol, 0.07 M dithiothreitol, 1% (w/v) SDS and 0.001% bromophenol blue. The samples were then pre-heated to 50 °C for 10 min and separated by SDS-PAGE by use of 4–12% Bis-Tris gels (Invitrogen, MD, USA), NuPAGE® MOPS SDS running buffer (Invitrogen, MD, USA) and Novex XCell II apparatus (Invitrogen, MD, USA). Protein bands were visualized by Coomassie Staining and molecular weight determined by use of Benchmark prestained protein ladder (Novex, Life technologies, 10 748–010) run simultaneously on the gel.

#### 2.3.4. Circular dichroism (CD)

The molecular conformation and denaturation temperature were assessed by CD spectra using a spectropolarimeter (Jasco J-810, Easton, MD, USA). Collagen was dissolved in 20 mM acetic acid to a concentration of 0.15 mg/ml and placed into a quartz cell with a path length of 1 mm. The spectrum from 180 to 250 nm was recorded with an interval of 0.5 nm and scanning speed of 50 nm/min under nitrogen atmosphere at 20 °C. To determine the denaturation temperature, the rotatory angle at a fixed wavelength of 221 nm was recorded with heating from 20 to 60 °C at a constant heating rate of 2 °C/min. The triple helix content of native collagen was adjusted to be 100%, and the value of the denaturated collagen to be 0%. Denaturation temperature was defined as the temperature that gave the midpoint of ellipticities between 20 and 60 °C.

#### 2.3.5. Nano differential scanning calorimetry (nano DSC)

Nano differential scanning calorimetry (nano DSC) experiments were performed using a Nano DSC 602 000 differential scanning calorimeter (TA Instruments, Lindon, UT, USA) with a capillary cell volume of 0.300 ml. DSC thermograms were recorded for 1.5 mg/ml collagen solutions in 20 mM acetic acid at a constant heating rate of 2 °C/min and 3 atm in the temperature range of 20–60 °C. Acetic acid (20 mM) was used as reference. The transition temperature of collagen was defined at the maximum of the transition peak after baseline subtraction. To assess the renaturation properties of the isolated collagen, the sample was dissolved in 20 mM acetic acid at 5 °C. The solution was heated to 55 °C, cooled to 5 °C and left in the nano DSC capillary cell for 2 weeks followed by heating to 55 °C. A sample stored at 4 °C was used as reference.

The results were processed by application of the NanoAnalyze software (TA Instruments). The partial specific heat capacity of collagen was determined from the estimated molecular weight and a partial specific volume of 0.700 ml/g (Noda, 1972). The results were fitted to a two-state trimer-to-monomer model. The deviation between the recorded data and the modulated data was $\leq$ 3%.

#### 2.3.6. Fourier transform infrared spectroscopy (FT-IR)

FT-IR spectra were acquired with a PerkinElmer Spotlight 400 FT-IR imaging system coupled to an optical IR spotlight microscope (PerkinElmer, Shelton, CO, USA). The sample (collagen) was placed on a ZnSe substrate and put under the microscope. The area selected for measurement was a thin part of the sample, approximately 5–10 µm thick. Single element absorbance spectra were recorded in the range from 4000 to 750 $cm^{-1}$ using a mercury cadmium telluride (MCT) detector, and with a spectral resolution of 4 $cm^{-1}$. For each pixel, 32 scans were obtained. The microscope was sealed with a custom-made box, and both microscope and spectrometer were purged with dry air to reduce the spectral contribution from water vapor and $CO_2$. A background spectrum/image of the ZnSe substrate was recorded before each sample measurement. The spectra were preprocessed by extended multiplicative signal corrections (EMSC) in The Unscrambler version 9.2 (Camo Process AS, Oslo, Norway) to remove multiplicative and wavenumber-independent and dependent baselines (Afseth and Kohler, 2012).

#### 2.3.7. Cell culture

Human primary dermal fibroblasts (ATCC, Manassas, VA, USA) were cultured in Dulbecco's modified Eagle's medium (DMEM) supplemented with 10% fetal bovine serum (FBS), 100 U/ml penicillin, 100 µg/ml streptomycin and 250 µg/ml fungizone in tissue culture flasks. The cells were maintained at 37 °C in a humidified atmosphere of 5% $CO_2$. The cells were routinely sub-cultivated twice a week. The cells were

examined by a Leica DM IL LED light microscope (Leica Microsystems Nussloch GmbH, Nuβloch, Germany) during incubation. Cells between passages 3–10 were used in these experiments.

#### 2.3.8. Cell viability

Evaluation of biocompatibility (viability) of collagen from turkey tendon was conducted for 48 h on proliferating cells. Fibroblasts were plated onto 96-well white opaque microtiter plates at a concentration of 3000 cells/well in medium with 2% FBS and incubated for approximately 24 h. The medium was then replaced with fresh medium. Collagen from turkey tendon was added to the wells in a concentration of 0.5, 1.0, 2.0 and 3.0 mg/ml and further incubated for 48 h. The samples were handled aseptic between isolation and the viability test. To mimic use under relevant biological conditions, the collagen was not dissolved before addition to the wells. Cell viability was measured with the Cell Titer-Glo Luminescent Cell Viability Assay (Promega, Madison, WI, USA) according to the manufacturer's protocol. The luminescence intensity was detected using a Synergy H1 Hybrid Multi-Mode Microplate Reader (Biotek, Bad Friedrichshall, Germany).

### 2.4. Preparation of drug loaded freeze dried scaffolds (sponges) of collagen from Turkey

Drug loaded freeze dried scaffolds of collagen i.e., collagen sponges, were prepared by a two-step gelation and crosslinking method. Prilocaine hydrochloride (PCL) was selected as a model drug ($M_w = 256.77$ g/mol). Collagen from turkey tendon was dissolved in 20 mM acetic acid over 24 h to a concentration of 5 mg/ml and filtered (5 μm Versapor® Membrane, Pall Corporation, MI, USA). PCL was mixed with the collagen solution to a final concentration of 5 mg/ml. The collagen-PCL solution was neutralized with 10X phosphate buffered saline (PBS) (0.1 × final volume) and 1 M NaOH (0.023 × volume of collagen solution) and diluted with Milli-Q water to a final concentration of 1X PBS and 2.5 mg/ml collagen. Riboflavin 5′-monophosphate sodium salt was added as a crosslinking agent to a final concentration of 0.01% (w/v) (Heo et al., 2016). The solution was incubated in the dark at 37 °C for 60 min to form intrahelical crosslinks and initiate gelling of the collagen. The collagen gels were irradiated with UVA ($\lambda_{max} = 365$ nm, 2.94 mW/cm$^2$) (Polylux-PT, Dreve, Germany), for 4 min to form interhelical crosslinks (i.e., a photochemically crosslinked gel). The crosslinking procedure was then completed by incubating the gels in the dark at 37 °C for 30 min. The non-irradiated gels were produced by mixing PCL with the collagen solution, addition of riboflavin, neutralization of the solution and incubation in the dark at 37 °C for 90 min.

All the gels were freeze dried in order to form sponges. The gels were frozen at −80 °C for 1 h prior to freeze drying at 0.0019 mbar for 20 h, including 1 h final drying at 0.0010 mbar (Alpha 2–4 LD Plus Freeze Fryer, Martin Christ, Germany).

### 2.5. Characterization of the drug loaded freeze dried scaffolds (sponges)

#### 2.5.1. In vitro release study of prilocaine hydrochloride from collagen sponges

Irradiated and non-irradiated collagen sponges were tested for *in vitro* release of the active ingredient (PCL). The study was performed using Franz diffusion cells (PermeGear, Hellertown, PA, USA). The diffusion area of the cell was 1.00 cm$^2$ and the receptor compartment had a capacity of 7.8 ml. Sink conditions were maintained.

Nylon membrane filters (0.45 μm Whatman™ Nylon membrane filters, GE Healthcare UK Ltd., Buckinghamshire, UK) were saturated with receptor medium (PBS) for 1 h prior to the experiment. The cells were filled with receptor medium and the membrane was mounted between the donor and the receptor compartment. The sponge was transferred from the container in which it was freeze dried to the donor chamber, and the container was rinsed with 1 ml Milli-Q water which was transferred to the donor chamber of the Franz cell. PCL was dissolved in PBS to a concentration of 5 mg/ml and 1 ml was added to the donor chamber of the Franz cell to serve as a positive control (a solution of the drug). The receptor medium was continuously stirred at 500 rpm. The receptor medium was kept at 32 ± 1 °C. Samples of 100 μl were withdrawn after 0.25, 0.33, 0.42, 0.5, 0.75, 1.0, 1.5, 2.0, 2.5, 3.0, 3.5, 4.0, 5.0, 6.0 and 24 h and diluted 1:1 with the HPLC mobile phase to a total volume of 200 μl. Fresh receptor medium was added to the receptor chamber to replace the sample volume withdrawn.

PLC was quantified by reversed-phase HPLC. The analysis was conducted with isocratic elution with a mobile phase consisting of 0.1 M acetate buffer pH 3.8 and methanol (60:40). A $C_{18}$ column (Nova-pak®, Waters Corporation, Milford, MA, USA) was used with a column temperature of 30 °C. The retention time of PCL at 1 ml/min flow was approximately 2.8 min under the given experimental conditions. All quantitative experiments were performed in triplicate unless otherwise stated.

#### 2.5.2. Environmental scanning electron microscopy (ESEM)

ESEM imaging of freeze dried collagen isolated from turkey tendon and sponges prepared from the isolated collagen was performed using an Environmental Scanning Electron Microscope (Zeiss EVO-50-EP, Carl Zeiss SMT Ltd, Coldhams Lane, Cambridge, UK). The samples were mounted on an aluminum stub using double-sided tape coated with carbon and coated with gold/palladium using a Sputter Coater (SC7640 Sputter Coater, Quorium Technologies).

#### 2.5.3. Mechanical properties

Mechanical properties of the derived sponges were studied using a TA-XT2i Texture Analyser (Stable Micro Systems, Haslemere, UK) in compression mode. The sponges were exposed to constant pressure at 0.1 mm/s to 10, 30 and 50% strain. The stress (kPa) was calculated by the force and load bearing area (A) of the sponges (r = 4 mm, A = 50.24 mm$^2$) and plotted against the strain.

#### 2.5.4. Thermogravimetric analysis (TGA)

Thermogravimetric analysis (TGA) were performed on the derived sponges using a TG 209F1 Libra (Netzsch-Gerätebau GmbH, Selb, Germany) under nitrogen purge (50 ml/min). TGA thermograms were recorded for samples between 5 and 10 mg at a constant heating rate of 10 °C/min in the temperature range 25–800 °C. The transition temperatures were defined as the onset temperature of the transition.

#### 2.5.5. Differential scanning calorimetry (DSC)

Differential scanning calorimetry (DSC) experiments were performed on the derived sponges using a DSC822$^e$ Differential Scanning Calorimeter (Mettler Toledo Intl. Inc., Greifensee, Switzerland) under dry nitrogen purge (80 ml/min). DSC thermograms were recorded for samples between 0.5 and 2 mg at a constant heating rate of 10 °C/min in the temperature range 25–400 °C. The samples were placed in aluminum sample pans with a pierced lid. An empty pan was used as reference. The transition temperature of collagen in the sponges was defined at the minimum of the transition peak when integrated.

### 2.6. Statistical analysis

The data was presented as mean ± highest deviation from three independent experiments. Statistical analyses were performed using Students t-test ($p < 0.05$).

## 3. Results and discussion

### 3.1. Characterization of collagen

#### 3.1.1. Total collagen quantification and estimated molecular weight

Collagen was isolated with pepsin in weak acetic acid. Pepsin is

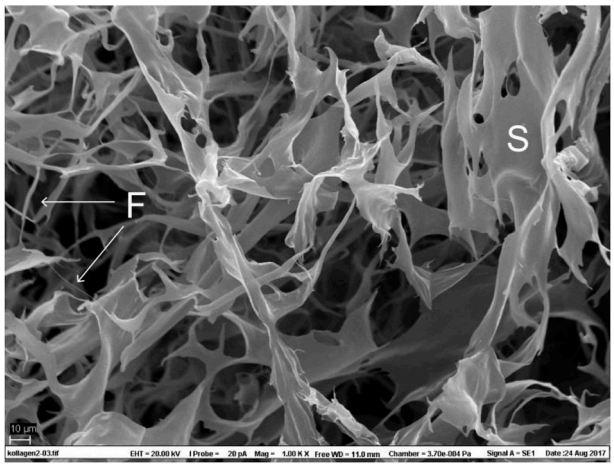


**Fig. 2.** ESEM image of freeze dried collagen extracted from turkey tendon at 1000X magnification (scale bar = 10 µm). Examples on collagen sheets and fibers are marked S and F, respectively.

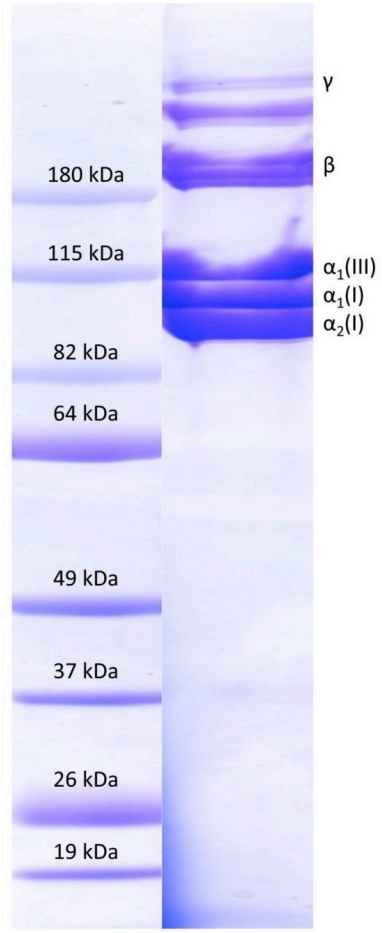


**Fig. 3.** SDS-PAGE of collagen from turkey tendon stained with Comassie Brilliant Blue. α, β and γ represent monomeric, dimeric and trimeric forms of the collagen molecules, respectively. Molecular weight standard (Benchmark prestained protein ladder) is shown to the left.

known to increase the yield of acid soluble crosslinked collagen and further to cleave the nonhelical telopeptide moieties of collagen, which leads to a product with good biocompatibility (Delgado et al., 2017). The purity of collagen was determined to 103.1 ± 3.1%, which indicated

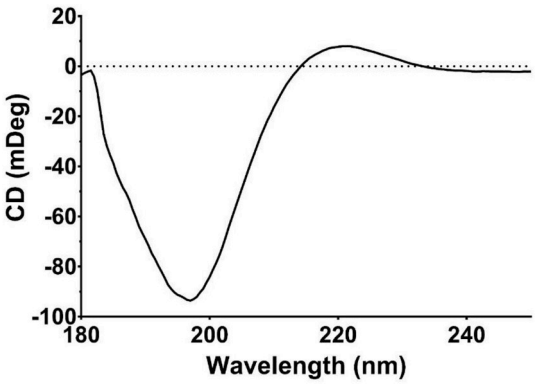


**Fig. 4.** CD spectrum of collagen from turkey tendon; 0.15 mg/ml in 20 mM acetic acid at 20 °C (50 nm/min). Rotary maximum = 221.5 nm, rotary minimum = 197 nm, crossover point = 214 nm.

that the isolated material solely consisted of collagen. The recovery of collagen was 95.7 ± 6.1% after filtration.

The intrinsic viscosity was found to be 19.76 dl/g. The average molecular weight was estimated to be 477.3 kDa. A standard collagen molecule is typically 300 kDa where each of the alpha strands are approximately 100 kDa (Shoulders and Raines, 2009). A higher molecular weight indicates the presence of interhelical crosslinks between the collagen molecules and formation of di- and trimers (Silver and Garg, 1997). The ESEM images of freeze dried pure collagen demonstrated the presence of both collagen sheets and fibers and confirmed the presence of interhelical crosslinks (Fig. 2).

### 3.1.2. SDS-PAGE pattern and CD spectroscopy of isolated collagen

The SDS-PAGE pattern indicated the presence of α-chains from both collagen type I and III (Rabotyagova et al., 2008; Han et al., 2018; Shikh Alsook et al., 2015) (Fig. 3). Different bands of high molecular weights around 115 kDa and above 180 kDa were detected. Previous SDS-gel electrophoresis studies of native collagen type I from tendon have revealed migration of reduced collagen type I into monomeric α1-and α2-chains in lower ranges approximately around 110 and 120, and β-band and γ-band above 240 kDa (Han et al., 2018; Rabotyagova et al., 2008; Shikh Alsook et al., 2015). Both types of collagen have previously been identified in tendons (Zhang et al., 2005).

The presence of β-dimers indicated intrahelical crosslinks between the collagen α-chains. The presence of γ-trimers indicated intrahelical crosslinking between the three collagen α-chains or intermolecular crosslinking between collagen molecules (Lewis and Piez, 1964). This is consistent with the high molecular weight as discussed above. ESEM analysis revealed fibrillary and sheet-like structures of freeze dried pure collagen supporting intermolecular crosslinks.

The CD spectrum of collagen showed a negative peak between 180 and 214 nm. The rotatory maximum was found at 221.5 nm, a minimum at 197 nm and a crossover point at 214 nm, which is characteristic for a triple helical conformation (Wang et al., 2014; Losso and Ogawa, 2014) (Fig. 4). This further emphasized the intact structure of isolated collagen.

### 3.1.3. Thermal properties of isolated collagen

The thermal denaturation of turkey collagen occurred in two steps with a minor transition ($T_s$) at 38.3 °C and a major transition ($T_m$) at 44.5 °C under the current experimental conditions (Fig. 5). The minor transition has previously been reported to be caused by collagen fibril depolymerization and melting of small parts of the triple helix structure, while the major transition was reported to be caused by denaturation of the triple helix to form monocoils (Liu et al., 2013). The transition at 44.5 °C was just above the turkey body temperature of 41.1 °C and is together with collagen from chicken keel bone among the highest

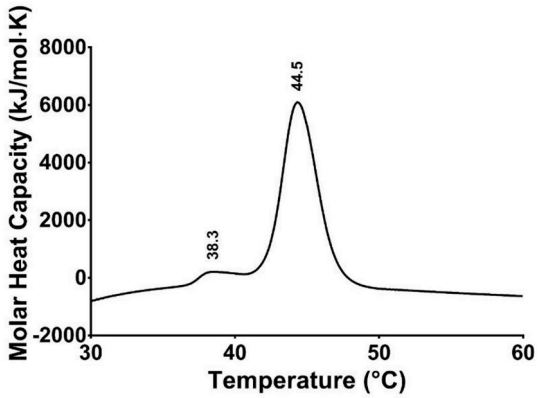


**Fig. 5.** Nano DSC thermogram of collagen from turkey tendon; 1.5 mg/ml in 20 mM acetic acid at heating rate 2 °C/min (baseline not subtracted).

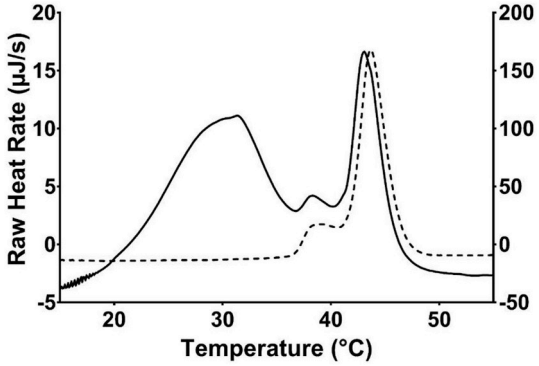


**Fig. 6.** Renaturation properties of collagen from turkey tendon (baseline subtracted). Left axis; partially renaturated collagen (solid line), right axis; collagen sample stored at 4 °C for the same time period (dashed line).

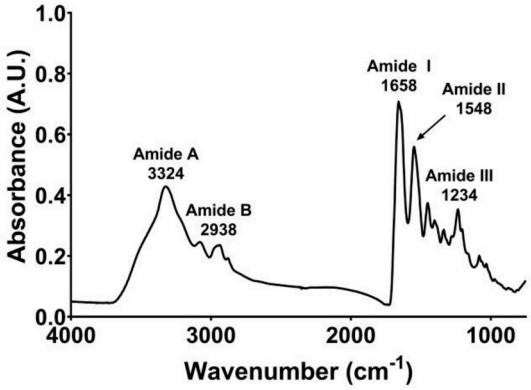


**Fig. 7.** FTIR spectrum of collagen from turkey tendon.

reported denaturation temperatures for collagen (Losso and Ogawa, 2014). A high denaturation temperature can be attributed to the imino acid content (hydroxyproline and hydroxylysine) of collagen (Persikov et al., 2005). However, the amino acid content was not investigated in detail in the present study. An extensive crosslinking of the collagen molecule can also contribute to a high denaturation temperature (Wright and Humphrey, 2002).

Two thermal transitions with $T_s$ between 36.1 and 38.4 °C and $T_m$ between 41.4 and 44.1 °C were observed in all samples (Fig. S1 A and B). The transition temperature for both transitions was dependent on the heating rate and shifted to a higher temperature when the heating rate increased. The transition temperature was a linear function of the logarithm of the heating rate (Figure S1 C). This indicated that the native protein was not in equilibrium with the unfolded protein, even at low heating rates (0.015 °C/min) and the unfolding was kinetically controlled (Liu et al., 2013). It is considered that such slow kinetics can be caused by a large activation energy or the many steps and complexity of the collagen unfolding (Leikina et al., 2002).

The helicity curve of collagen (Fig. S2) showed a biphasic transition, which is consistent with the two transitions from the nano DSC experiments (Fig. 5). The helicity went from 100% to 0% during the temperature interval 37–47 °C, which matched the onset temperature of the minor transition and offset temperature of the major transition, respectively, in the nano DSC experiments and confirmed the high denaturation temperature.

Collagen melting and denaturation has been described both as an irreversible rate-limited process with first-order reaction kinetics and Arrhenius dependency, and as a reversible process with an apparent irreversibility due to extremely slow equilibrium kinetics (Leikina et al., 2002). Lumry and Eyring (1954) proposed a three-state model for the thermal denaturation of proteins, involving a thermodynamic step and a kinetically controlled step (Equation (2)):

$$N \leftrightarrow U \rightarrow D \quad (2)$$

where N is the protein in its native form, U is the unfolded triple helix form and D is the denaturated form of the protein (Lumry and Eyring, 1954). This model has been evaluated to be the best model for the thermal denaturation of collagen (Liu and Li, 2010). The minor transition observed in the thermogram of collagen can thereby be assigned to the reversible step, while the major transition can be assigned the irreversible denaturation step in the Lumry-Eyring model (Liu et al., 2013).

According to Leikina et al., (2002) the peak transition temperature below 44.5 °C, i.e., $T_m$ of collagen, is related to formation of gelatin fragments. Partial refolding of collagen with formation of gelatin fragments was demonstrated by a renaturation study (Fig. 6). The refolding capability was apparently maintained even when the sample was heated to 55 °C. Irreversible refolding of collagen has been reported when the molecule is heated above 55 °C (Liu et al., 2013). Temperatures above this value could be avoided in a pharmaceutical context unless heating is the only option for sterilization (Wright and Humphrey, 2002).

### 3.1.4. FT-IR analysis

The FT-IR spectrum of the isolated collagen included the bands of amide A (3324 $cm^{-1}$), amide B (2938 $cm^{-1}$), amide I (1658 $cm^{-1}$), amide II (1548 $cm^{-1}$) and amide III (1234 $cm^{-1}$) (Fig. 7).

The amide A band of collagen has been associated with the NH-stretching frequency and is usually found at 3325-3330 $cm^{-1}$. The position is shifted towards a lower frequency, around 3300 $cm^{-1}$, if the NH group of a protein or peptide is involved in a hydrogen bond (Doyle et al., 1975). However, NH-stretching occuring in the range 3400–3440 $cm^{-1}$ indicates a free NH group (Wang et al., 2014). Collagen from turkey tendon was found to have an amide A band at 3324 $cm^{-1}$, which was an indication of hydrogen bonding (Doyle et al., 1975). The amide B band position of collagen from turkey tendon was observed at 2938 $cm^{-1}$. This band could be related to the asymmetrical stretch of $CH_2$ (Fauzi et al., 2016).

The amide I, II and III bands are related to the secondary polypeptide conformation of proteins. The amide I band of collagen has previously been reported at 1650-1688 $cm^{-1}$ (Doyle et al., 1975). In the present study the amide I band was identified at 1658 $cm^{-1}$, which indicated the existence of non-equivalent C=O bonds. The band was asymmetrical, which is typical for collagens (Terzi et al., 2018). The amide II band of collagen is usually found at 1530-1540 $cm^{-1}$, however, if the material is partially hydrated, the band moves to higher frequencies around 1550 $cm^{-1}$ (Doyle et al., 1975). The present collagen was found to have an amide II band at 1548 $cm^{-1}$, which further indicated a partially hydrated material. The amide II band is associated with N–H bend coupled

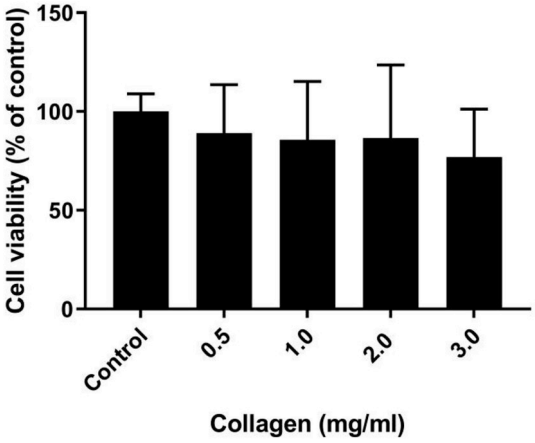


**Fig. 8.** Viability (i.e. the amount of ATP present) of human primary dermal fibroblasts treated with different collagen concentrations and without (control). The data is presented as the mean of three independent cell culture experiments seeded out in triplicates.

with C–N stretching. The amide III band of collagen is associated with N–H bend coupled with C–N stretch and indicates the presence of a helical structure. The amide III bands in our samples were identified around 1234 $cm^{-1}$ and confirmed the native structure of the collagen triple helix (Terzi et al., 2018; Gąsior-Głogowska et al., 2010).

*3.1.5. In vitro biocompatibility assessment of isolated collagen*

The addition of collagen to primary human fibroblasts did not significantly affect the cell viability (i.e., the amount of ATP present) after 48 h at any of the concentrations of the isolated collagen compared to the control (Fig. 8). However, the viability showed a slight decrease with increasing collagen concentration. Collagen is supposed to be biocompatible and non-toxic to cells. The variance in the results can therefore be attributed to the increasing bulk volume of collagen in the well and/or a quenching of the luminescence from the luciferase in the viability assay. The results demonstrated good *in vitro* biocompatibility of the isolated collagen at concentrations relevant for production of freeze dried scaffolds.

*3.2. Characterization of collagen freeze dried scaffolds (sponges)*

*3.2.1. Mechanical properties*

Freeze dried scaffolds prepared in the presence or absence of photo-crosslinking resulted in sponges with different mechanical properties. The mechanical property studies of the sponges showed a clear difference between the stress at 10, 30 and 50% strain of the irradiated and non-irradiated sponges, respectively. The irradiated sponges had a stress varying between $1.35 \pm 0.72$ kPa at 10% strain, $2.08 \pm 0.58$ kPa at 30% strain and $3.74 \pm 0.94$ kPa at 50% strain. The non-irradiated sponges had a stress varying between $0.22 \pm 0.03$ kPa at 10% strain, $0.77 \pm 0.17$ kPa at 30% strain and $1.79 \pm 0.20$ kPa at 50% strain (Fig. 9 A and B). The variance within the irradiated samples can be attributed to an inhomogeneous photochemical crosslinking throughout the sample, due to a filter effect. This can in the future be addressed by making thinner sponges with a larger irradiation surface area. The flattening of the curve, especially for the irradiated sponges at strain $\geq$ 30%, can be attributed to the bending of the sponge, rather than direct compression. This happened to all the irradiated sponge samples at $>$ 30% strain. Upon dispersion in aqueous solution, the irradiated sponges retained their structure, while the non-irradiated sponges disintegrated.

*3.2.2. Thermal stability of collagen sponges*

Thermal stability studies of the two different sponges by TGA showed a significant weight loss with onset at approximately 173 °C and a small weight loss with onset at approximately 285 °C. The major weight loss was ascribed to PCL, while the small weight loss was ascribed to the decomposition of collagen (Fig. S3) (Schmidt et al., 2004; Ashokkumar et al., 2016). The results showed no differences in the thermal stability between the samples. However, the DSC results revealed differences with the irradiated sponges exhibiting a transition at $63.5 \pm 2.5$ °C compared to the non-irradiated sponges with a very weak transition at $57.1 \pm 1.9$ °C (Fig. S4). The transition corresponds to a shrinkage and the loss of the triple helical structure of collagen (Ashokkumar et al., 2016; Pietrucha, 2005). The transition around 40 °C was ascribed to PCL.

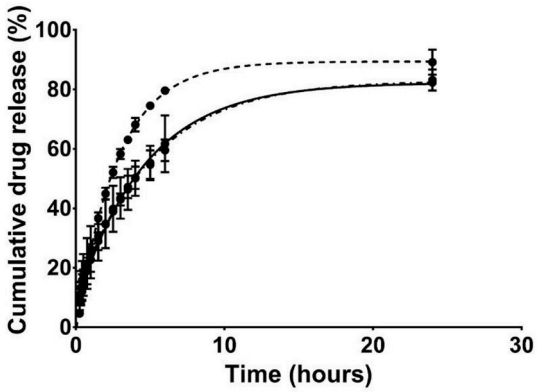


**Fig. 10.** *In vitro* release curves of prilocaine hydrochloride from irradiated collagen sponges (solid line), non-irradiated collagen sponges (dash-dotted line) and a solution of the drug (dashed line). The first two curves are superimposed.

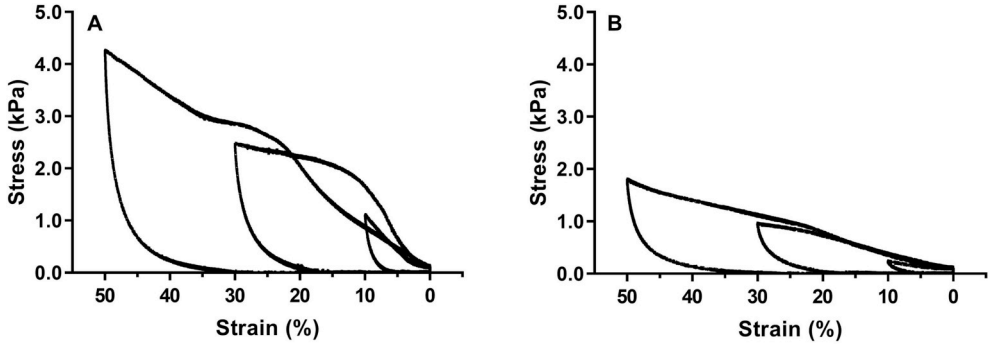


**Fig. 9.** Representative figures of compressive stress-strain curves of collagen sponges at 10, 30 and 50% strain. A: irradiated collagen sponges, B: non-irradiated collagen sponges.

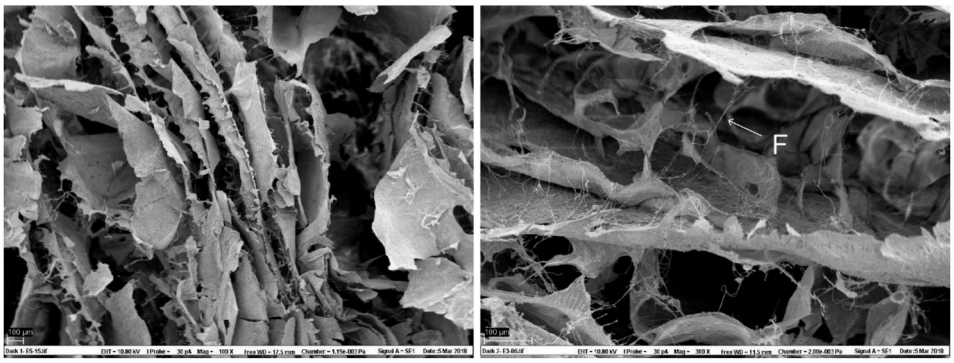


**Fig. 11.** Cross section of non-irradiated collagen sponges at 100X (left) and 300X (right) magnification (scale bars = 100 μm). The images show collapsed pore structures and few fibrils (F) to stabilize the pores.

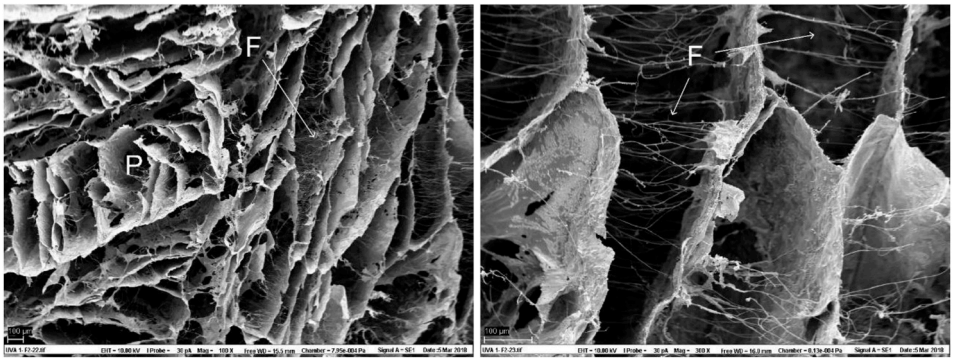


**Fig. 12.** Cross section of irradiated collagen sponges at 100X (left) and 300X (right) magnification (scale bars = 100 μm). The images show formation of more and smaller pores (P) compared to the non-irradiated sponges. The right image shows formation of fibrils (F) stabilizing the pores.

### 3.2.3. *In vitro release study of prilocaine hydrochloride from collagen sponges*

There was a significant slower release of PCL from the sponges compared to the membrane passage of a solution of the drug (Fig. 10). The difference between irradiated and non-irradiated sponges was however, not significant. The sustained release of the model drug from the sponge can be explained by diffusion through the hydrogel that was formed upon hydration of the sponge (Li and Mooney, 2016; Tihan et al., 2016). The slower release achieved from the sponges can be beneficial for applications where a prolonged effect of the active ingredient is requested, like a pain-relieving agent or a local anesthetic like our model drug. For other types of drugs, e.g. a photosensitizer for localized antimicrobial photodynamic therapy, a fast release will be desired. PCL is water soluble and can easily be quantified with a chromatographic method. PCL and riboflavin have no overlap in their respective absorption spectra. PCL was regarded as stable under the applied polymerization conditions, i.e., the degradation was $\leq$6%, and the substance served as a relevant and convenient model drug in the current experiments.

### 3.2.4. *Morphology of collagen sponges*

The ESEM images and structure of the sponge indicated that the degree of crosslinking was higher for the irradiated sponges than the non-irradiated sponges due to the photopolymerization of collagen fibrils in the presence of riboflavin (Figs. 11 and 12). The irradiated material showed a more rigid structure. The pores formed by crosslinking were probably too large to retain and control the release of the selected model drug which is a small molecule with $M_w = 256.8$ g/mol. During freeze drying, ice grows into large crystals, segregating the solute and compress it into thin sheets. Once the ice sublimate, empty spaces (i.e., pores) are formed. The pore size and mechanical properties of the collagen sponges could be altered by increasing the collagen concentration and/or change the polymerization conditions (Tirella et al., 2012). This was, however, not performed in the current study, but will be investigated as the next step. The pore size and scaffold architecture will directly affect the mechanical stability of the scaffold and behavior of cells migrating into the device. Cell migration is dependent on that the specific surface area of the scaffold is large enough for cells to attach, e.g. a high number of pores per unit area. However, the pores must be large enough to facilitate cell migration and cell nutrition exchange. The pore size estimated from the ESEM images of irradiated sponges was within the optimal pore size reported in the literature for cell attachment and proliferation (approximately 250–500 μm) (Murphy and O'Brien, 2010; Loh and Choong, 2013; Davidenko et al., 2015). It might therefore be difficult to achieve a pore size small enough to obtain controlled release of low-molecular weight probes ($\approx$ 500 g/mol), but sponges for controlled release of larger molecules, polymeric compounds, peptides and proteins could be achieved by an optimization of the production method.

## 4. Conclusions

Collagen of high purity was isolated from turkey tendons by application of acetic acid and pepsin. The collagen was identified as type I and III. CD and FT-IR studies confirmed that the native triple helix structure was preserved after isolation. The collagen demonstrated high thermal stability, among the highest reported for vertebras, and good biocompatibility. An *in vitro* release test showed promising results for the application of freeze dried collagen scaffolds as a drug delivery system. There was a significant difference between the release rate of the model drug from the sponges and from a solution. Photochemical polymerization of the sponges increased the mechanical properties and made the product easier to handle. The properties of the isolated material and of the preliminary formulations make this collagen a

promising candidate as excipient in pharmaceutical as well as cosmetic products.

## Acknowledgments

The authors are grateful to Bente Amalie Breiby, Tove Larsen and Julia Fredrika Alopaeus, Department of Pharmacy, University of Oslo, Per Eugen Kristiansen, Department of Biosciences, University of Oslo, Ingrid Marie Bergh Bakke, Department of Chemistry, University of Oslo and Ragnhild Stenberg Berg, Nofima AS for technical support. Turkey tendon by-products and financial support for isolation of collagen from turkey were contributed by Norilia AS. The ESEM instrument was borrowed from the Imaging Centre of the Norwegian University of Life Sciences.

## Appendix A. Supplementary data

Supplementary data to this article can be found online at https://doi.org/10.1016/j.scp.2019.100166.

## Conflicts of interest

The authors declare that they have no conflict of interest.

## Funding

This work was supported by Norilia AS (Oslo, Norway).

## Disclosure statement

*Conceptualization*: K. G. Grønlien, M. E. Pedersen, J. Karlsen, H. H. Tønnesen.

*Funding acquisition*: J. Karlsen.

*Investigation*: K. G. Grønlien, K. W. Sanden, V. Høst.

*Supervision*: M. E. Pedersen, J. Karlsen, H. H. Tønnesen.

*Visualization:* K. G. Grønlien, V. Høst.

*Writing*: K. G. Grønlien, M. E. Pedersen, K. W. Sanden, V. Høst, J. Karlsen, H. H. Tønnesen.

Norilia AS provided the turkey tendon by-products and funded the isolation of collagen and kits for analysis of collagen, but was not involved in the study design, interpretation of the data, writing of the manuscript, or decision to publish.

## References

Afseth, N.K., Kohler, A., 2012. Extended multiplicative signal correction in vibrational spectroscopy, a tutorial. Chemometr. Intell. Lab. 117, 92–99.

Ashokkumar, M., Cristian Chipara, A., Tharangattu Narayanan, N., Anumary, A., Sruthi, R., Thanikaivelan, P., Vajtai, R., Mani, S.A., Ajayan, P.M., 2016. Three-dimensional porous sponges from collagen biowastes. ACS Appl. Mater. Interfaces 8, 14836–14844.

Chattopadhyay, S., Raines, R.T., 2014. Collagen-based biomaterials for wound healing. Biopolymers 101, 821–833.

Cliche, S., Amiot, J., Avezard, C., Gariepy, C., 2003. Extraction and characterization of collagen with or without telopeptides from chicken skin. Poult. Sci. 82, 503–509.

Davidenko, N., Schuster, C.F., Bax, D.V., Raynal, N., Farndale, R.W., Best, S.M., Cameron, R.E., 2015. Control of crosslinking for tailoring collagen-based scaffolds stability and mechanics. Acta Biomater. 25, 131–142.

Delgado, L.M., Shologu, N., Fuller, K., Zeugolis, D.I., 2017. Acetic acid and pepsin result in high yield, high purity and low macrophage response collagen for biomedical applications. Biomed. Mater. 12, 065009.

Desimone, M.F., Hélary, C., Quignard, S., Rietveld, I.B., Bataille, I., Copello, G.J., Mosser, G., Giraud-Guille, M.-M., Livage, J., Meddahi-Pellé, A., Coradin, T., 2011. In vitro studies and preliminary in vivo evaluation of silicified concentrated collagen hydrogels. ACS Appl. Mater. Interfaces 3, 3831–3838.

Doyle, B.B., Bendit, E.G., Blout, E.R., 1975. Infrared spectroscopy of collagen and collagen-like polypeptides. Biopolymers 14, 937–957.

Farndale, R.W., 2006. Collagen-induced platelet activation. Blood Cells Mol. Dis. 36, 162–165.

Fauzi, M.B., Lokanathan, Y., Aminuddin, B.S., Ruszymah, B.H.I., Chowdhury, S.R., 2016. Ovine tendon collagen: extraction, characterisation and fabrication of thin films for tissue engineering applications. Mater. Sci. Eng. C 68, 163–171.

Gąsior-Głogowska, M., Komorowska, M., Hanuza, J., Ptak, M., Kobielarz, M., 2010. Structural alteration of collagen fibres - spectroscopic and mechanical studies. Acta Bioeng. Biomech. 12, 55–62.

Han, L., Zhang, Z.W., Wang, B.H., Wen, Z.K., 2018. Construction and biocompatibility of a thin type I/II collagen composite scaffold. Cell Tissue Bank. 19, 47–59.

Heo, J., Koh, R., Shim, W., Kim, H., Yim, H.-G., Hwang, N., 2016. Riboflavin-induced photo-crosslinking of collagen hydrogel and its application in meniscus tissue engineering. J. Control. Release 6, 148–158.

Jayathilakan, K., Sultana, K., Radhakrishna, K., Bawa, A.S., 2012. Utilization of byproducts and waste materials from meat, poultry and fish processing industries: a review. J. Food Sci. Technol. 49, 278–293.

Kane, R.J., Weiss-Bilka, H.E., Meagher, M.J., Liu, Y., Gargac, J.A., Niebur, G.L., Wagner, D.R., Roeder, R.K., 2015. Hydroxyapatite reinforced collagen scaffolds with improved architecture and mechanical properties. Acta Biomater. 17, 16–25.

Kulicke, W.-M., Clasen, C., 2004. Viscosimetry of Polymers and Polyelectrolytes. Springer, Berlin.

Leikina, E., Mertts, M.V., Kuznetsova, N., Leikin, S., 2002. Type I collagen is thermally unstable at body temperature. Proc. Natl. Acad. Sci. U.S.A. 99, 1314–1318.

Lewis, M.S., Piez, K.A., 1964. Sedimentation-equilibrium studies of the molecular weight of single and double chains from rat-skin collagen. Biochemistry 3, 1126–1131.

Li, H., Liu, B.L., Gao, L.Z., Chen, H.L., 2004. Studies on bullfrog skin collagen. Food Chem. 84, 65–69.

Li, J., Mooney, D.J., 2016. Designing hydrogels for controlled drug delivery. Nat. Rev. Mater. 1, 16071.

Liu, W., Li, G., 2010. Non-isothermal kinetic analysis of the thermal denaturation of type I collagen in solution using isoconversional and multivariate non-linear regression methods. Polym. Degrad. Stab. 95, 2233–2240.

Liu, Y., Liu, L., Chen, M., Zhang, Q., 2013. Double thermal transitions of type I collagen in acidic solution. J. Biomol. Struct. Dyn. 31, 862–873.

Loh, Q.L., Choong, C., 2013. Three-dimensional scaffolds for tissue engineering applications: role of porosity and pore size. Tissue Eng. B Rev. 19, 485–502.

Losso, J.N., Ogawa, M., 2014. Thermal stability of chicken keel bone collagen. J. Food Biochem. 38, 345–351.

Lumry, R., Eyring, H., 1954. Conformation changes of proteins. J. Phys. Chem. 58, 110–120.

Murphy, C.M., O'Brien, F.J., 2010. Understanding the effect of mean pore size on cell activity in collagen-glycosaminoglycan scaffolds. Cell Adhes. Migrat. 4, 377–381.

Nishihara, T., Doty, P., 1958. The sonic fragmentation of collagen macromolecules. Proc. Natl. Acad. Sci. U.S.A. 44, 411–417.

Noda, H., 1972. Partial specific volume of collagen. J. Biochem. 71, 699–703.

Pantin-Jackwood, M.J., Stephens, C.B., Bertran, K., Swayne, D.E., Spackman, E., 2017. The pathogenesis of H7N8 low and highly pathogenic avian influenza viruses from the United States 2016 outbreak in chickens, turkeys and mallards. PLoS One 12, e0177265.

Parenteau-Bareil, R., Gauvin, R., Cliche, S., Gariepy, C., Germain, L., Berthod, F., 2011. Comparative study of bovine, porcine and avian collagens for the production of a tissue engineered dermis. Acta Biomater. 7, 3757–3765.

Persikov, A.V., Ramshaw, J.A.M., Brodsky, B., 2005. Prediction of collagen stability from amino acid sequence. J. Biol. Chem. 280, 19343–19349.

Pietrucha, K., 2005. Changes in denaturation and rheological properties of collagen–hyaluronic acid scaffolds as a result of temperature dependencies. Int. J. Biol. Macromol. 36, 299–304.

Postlethwaite, A.E., Seyer, J.M., Kang, A.H., 1978. Chemotactic attraction of human fibroblasts to type I, II, and III collagens and collagen-derived peptides. Proc. Natl. Acad. Sci. U.S.A. 75, 871–875.

Prinzinger, R., Preßmar, A., Schleucher, E., 1991. Body temperature in birds. Comp. Biochem. Physiol. A: Physiol. 99, 499–506.

Rabotyagova, O.S., Cebe, P., Kaplan, D.L., 2008. Collagen structural hierarchy and susceptibility to degradation by ultraviolet radiation. Mater. Sci. Eng. C 28, 1420–1429.

Rider, P., Kačarević, Ž.P., Alkildani, S., Retnasingh, S., Barbeck, M., 2018. Bioprinting of tissue engineering scaffolds. J. Tissue Eng. 9, 2041731418802090-90.

Schmidt, A.C., Niederwanger, V., Griesser, U.J., 2004. Solid-state forms of prilocaine hydrochloride. J. Therm. Anal. Calorim. 77, 639–652.

Shikh Alsook, M.K., Gabriel, A., Salouci, M., Piret, J., Alzamel, N., Moula, N., Denoix, J. M., Antoine, N., Baise, E., 2015. Characterization of collagen fibrils after equine suspensory ligament injury: an ultrastructural and biochemical approach. Vet. J. 204, 117–122.

Shoulders, M.D., Raines, R.T., 2009. Collagen structure and stability. Annu. Rev. Biochem. 78, 929–958.

Silver, F.H., Garg, A.K., 1997. Collagen: characterization, processing and medical applications. In: Domb, A.J., Kost, J., Wiseman, D.M. (Eds.), Handbook of Biodegradable Polymers. Harwood Academic Publishers, Amsterdam, pp. 323–350.

Sotelo, C.G., Comesaña, M.B., Ariza, P.R., Pérez-Martín, R.I., 2016. Characterization of collagen from different discarded fish species of the west coast of the iberian peninsula. J. Aquat. Food Prod. Technol. 25, 388–399.

Telay Mekonnen, B., Meiyazhagan, A., Ragothaman, M., Kalirajan, C., Palanisamy, T., 2019. Bi-functional iron embedded carbon nanostructures from collagen waste for photocatalysis and Li-ion battery applications: a waste to wealth approach. J. Clean. Prod. 210, 190–199.

Terzi, A., Storelli, E., Bettini, S., Sibillano, T., Altamura, D., Salvatore, L., Madaghiele, M., Romano, A., Siliqi, D., Ladisa, M., De Caro, L., Quattrini, A., Valli, L., Sannino, A., Giannini, C., 2018. Effects of processing on structural, mechanical and biological properties of collagen-based substrates for regenerative medicine. Sci. Rep. 8, 1429.

Tihan, G.T., Rău, I., Zgârian, R.G., Ghica, M.V., 2016. Collagen-based biomaterials for ibuprofen delivery. C. R. Chim. 19, 390–394.
Tirella, A., Liberto, T., Ahluwalia, A., 2012. Riboflavin and collagen: new crosslinking methods to tailor the stiffness of hydrogels. Mater. Lett. 74, 58–61.
Varriale, A., Bernardi, G., 2006. DNA methylation and body temperature in fishes. Gene 385, 111–121.
Wang, L., Liang, Q., Chen, T., Wang, Z., Xu, J., Ma, H., 2014. Characterization of collagen from the skin of Amur sturgeon (Acipenser schrenckii). Food Hydrocolloids 38, 104–109.
Wilson, W.O., Woodard, A., 1955. Some factors affecting body temperature of turkeys. Poult. Sci. 34, 369–371.
Wright, N.T., Humphrey, J.D., 2002. Denaturation of collagen via heating: an irreversible rate process. Annu. Rev. Biomed. Eng. 4, 109–128.
Yousefi, M., Ariffin, F., Huda, N., 2017. An alternative source of type I collagen based on by-product with higher thermal stability. Food Hydrocolloids 63, 372–382.
Zhang, G., Young, B.B., Ezura, Y., Favata, M., Soslowsky, L.J., Chakravarti, S., Birk, D.E., 2005. Development of tendon structure and function: regulation of collagen fibrillogenesis. J. Musculoskelet. Neuronal Interact. 5, 5–21.